

Ongoing Development of the Bass Strait GNSS/INS Buoy System for Altimetry Validation in Preparation for SWOT

Boye Zhou ^{1,*}, Christopher Watson ^{1,2}, Benoit Legresy ^{2,3}, Matt A. King ¹ and Jack Beardsley ²

¹ School of Geography, Planning, and Spatial Sciences, University of Tasmania, Hobart, Tasmania 7001, Australia

² Integrated Marine Observing System, Hobart, Tasmania 7004, Australia

³ Commonwealth Scientific and Industrial Research Organisation, Oceans and Atmosphere, Hobart, Tasmania 7004, Australia

* Correspondence: boye.zhou@utas.edu.au

1. Contents

- Introduction
- Table S1 Processing Strategies for DD and PPP
- Table S2 Outlier Percentage of B–M Residual for Each Deployment
- Figure S1 Watch Circle and Horizontal Movement of the Buoy for Deployment 66
- Figure S2 RMS of B–M Residual as a Function of Filtering Window Length
- Figure S3 Schematic Illustration of Buoy Dynamics under Impact of External Forcings
- Figure S4 Schematic Derivation of Buoy Acceleration from INS
- Figure S5 Schematic Derivation of Buoy Acceleration from GNSS
- Figure S6 B–M Residual from PPP processing
- Figure S7 Profile of Buoy Dynamics for Deployment 63
- Figure S8 Profile of Buoy Dynamics for Deployment 64
- Figure S9 Profile of Buoy Dynamics for Deployment 65

2. Introduction

This supplementary material includes the detailed processing strategies we used for differential processing via TRACK and PPP via GipsyX (Table S1). Outlier percentage of B–M residual for each deployment is detailed in Table S2. It also includes the horizontal movement of the buoy and a fitted watch circle for deployment 66 (Figure S1). Figure S2 shows the result of the investigation into the optimal filtering window length for the buoy solutions. Schematic illustration of the buoy dynamics under the impact of the external forcings is shown in Figure S3. Two schematics are provided to show the derivation of buoy acceleration from INS and GNSS (Figure S4, Figure S5) Furthermore, B–M residual from PPP processing of four deployments used in this study is provided in Figure S6. Finally, the profiles of buoy dynamics for deployment 63 to 65 are provided in Figure S7, Figure S8 and Figure S9 respectively.

Citation: Zhou, B.; Watson, C.; Legresy, B.; King, M.A.; Beardsley, J. Ongoing Development of the Bass Strait GNSS/INS Buoy System for Altimetry Validation in Preparation for SWOT. *Remote Sens.* **2023**, *15*, 287. <https://doi.org/10.3390/rs15010287>

Academic Editors: Xiaoli Deng, Jérôme Benveniste and Stelios Mertikas

Received: 8 November 2022

Revised: 16 December 2022

Accepted: 22 December 2022

Published: 3 January 2023



Copyright: © 2023 by the authors. Licensee MDPI, Basel, Switzerland. This article is an open access article distributed under the terms and conditions of the Creative Commons Attribution (CC BY) license (<https://creativecommons.org/licenses/by/4.0/>).

Table S1. Processing Strategies for DD and PPP respectively in TRACK and GipsyX

<i>GNSS Processing</i>	<i>DD (TRACK)</i>	<i>PPP (GipsyX)</i>
<i>Frequencies</i>	L1 + L2	
<i>Coordinate Constraints</i>	1 m/ $\sqrt{\text{sec}}$ for base 2 m/ $\sqrt{\text{sec}}$ for rover	2 m / sqrt(sec)
<i>Single Session Length</i>	7 hours	7 hours
<i>Cut-off Angle</i>	10 degrees	10 degrees
<i>Tropospheric Model</i>	VMF3 with a priori of 0.1 m constraint: 0.01 mm/ $\sqrt{\text{sec}}$	VMF1
<i>Ionosphere Handling</i>	Iono-Free Combination	
<i>DCB Correction</i>	GPS+GLONASS	GPS
<i>PCV Correction</i>	GPS+GLONASS Applied with INS integration	GPS (no INS)
<i>Ambiguity Fixing</i>	GPS Integer GLONASS Float	GPS Integer
<i>Clock & Orbit</i>	GFZ 15-min product	JPL 30-sec product
<i>Solid Earth Tide</i>	IERS 2010 Convention	
<i>Ocean Tide Loading</i>	FES2014b with CM correction via IERS 2010 Convention	
<i>Relativistic Corrections</i>	Applied (to 2 nd order)	–
<i>ARP Correction</i>	Applied with INS integration	–
<i>Phase Wrap-Up</i>	Applied with INS integration	–
<i>Additional Product</i>	–	JPL Wide-Lane Phase Bias Product

Table S2. Outlier Percentage for the deployments considered. For deployment 65, no valid solution from PPP is generated yet – still under investigation of possible data quality issue.

	Double Differencing	Precise Point Positioning
Deployment 63	11.2%	17.1%
Deployment 64	5.6%	9.1%
Deployment 65	6.0%	–
Deployment 66	8.4%	2.0%

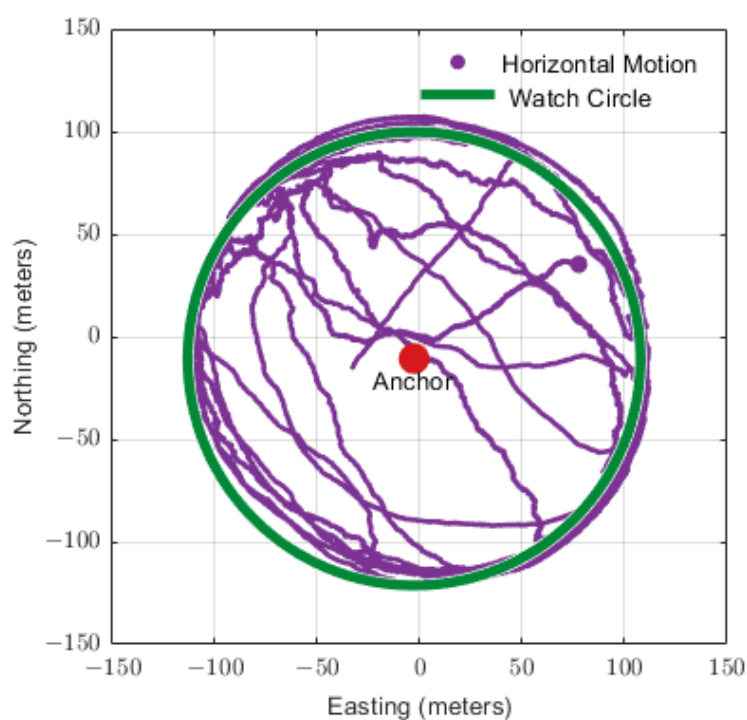


Figure S1. Watch Circle and Horizontal Movement of the Buoy for Deployment 66. The purple line describes the route of buoy during deployment 66. Red point in the middle indicates the location of the anchor point. The green solid line is a fitted watch circle for the buoy, approximating an outer bound of the horizontal movement of the buoy.

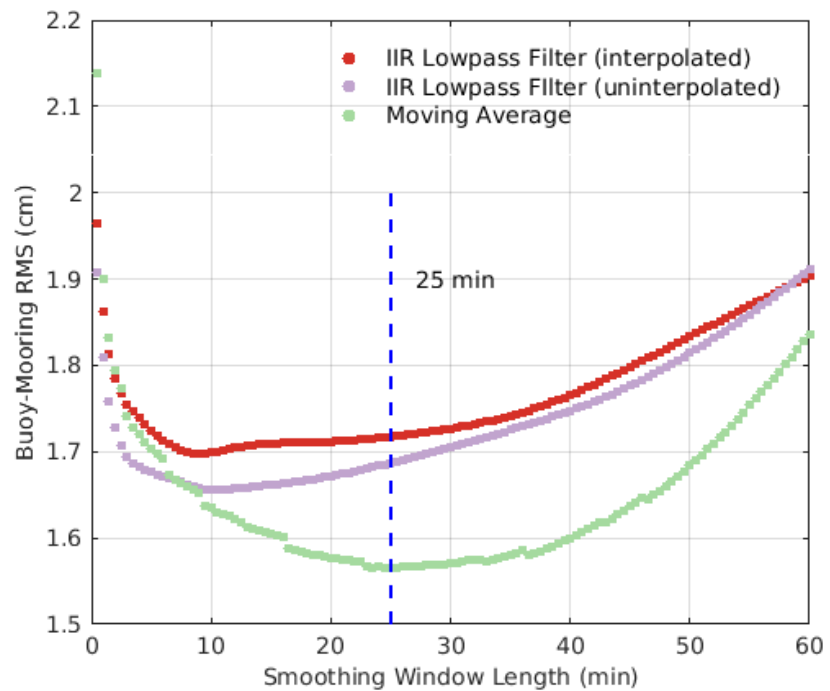


Figure S2. RMS of B–M Residual as a Function of Filtering Window Length. Three sets of lowpass filters were investigated: Infinite Impulse Response (IIR) lowpass filters (e.g., Butterworth, Chebyshev, Bessel, Elliptic) on series with interpolated values leaving no gaps; IIR lowpass filters on uninterpolated series with gaps; moving average on series with gaps. Results show that the RMS of the B–M residual across 27 deployments from 2012 to 2018 dropped to its minimum around a window of 25 min using moving average filter, which drives our choice of a 25-min moving mean method used for the buoy solutions.

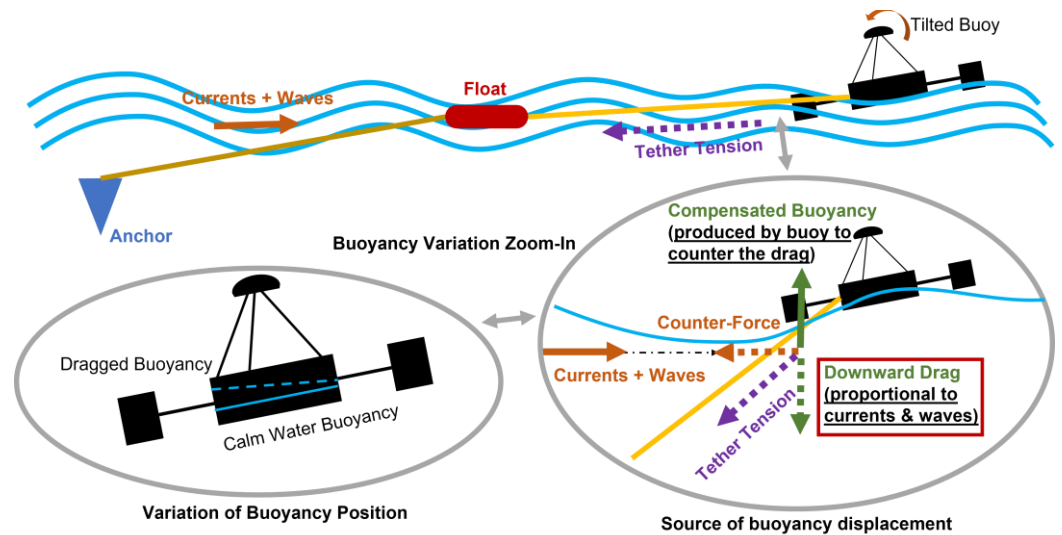


Figure S3. Schematic Illustration of Buoy Dynamics under the Impact of External Forcings

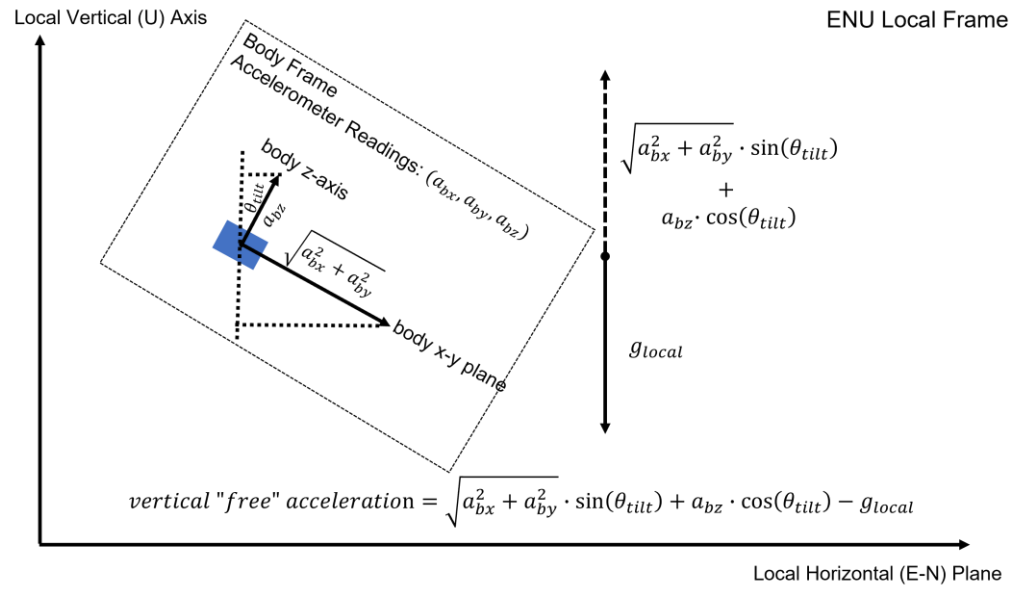


Figure S4. Schematic Derivation of Buoy Acceleration from INS. Following basic trigonometry, vertical acceleration of the buoy excluding the local gravity (defined as “free” acceleration) in the local frame (ENU) can be calculated using the body frame accelerometer readings (a_{bx}, a_{by}, a_{bz}) by the IMU and the buoy tilt θ_{tilt} derived from the Attitude and Heading Reference System (AHRS) filter.

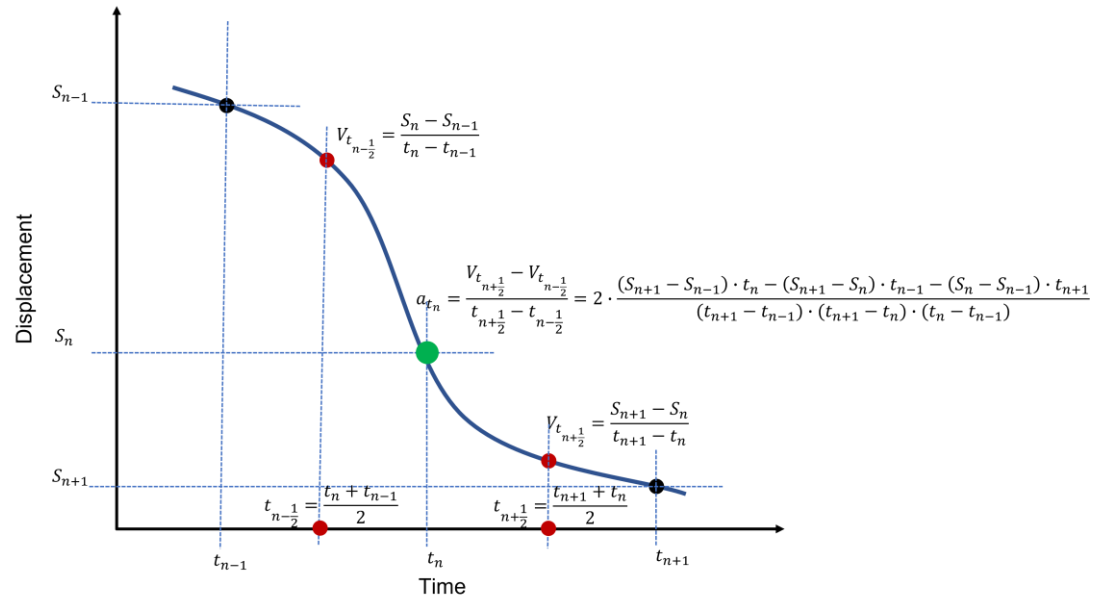


Figure S5. Schematic Derivation of Buoy Acceleration from GNSS. Basic velocity and acceleration formulae are used to derive the buoy acceleration at a given epoch.

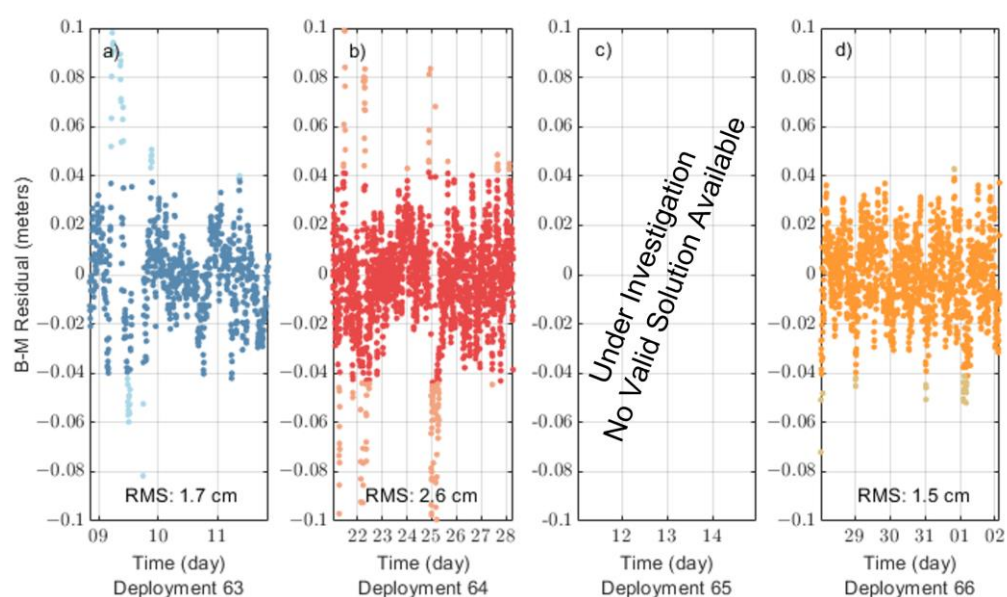


Figure S6. B–M Residual from PPP processing. From Panel (a) to (d) shows respectively the residual for deployment 63, 64, 65 and 66. It can be seen that SSH solutions from deployment 63 and 64 suffered from processing quality, while for deployment 65, no solution of proper quality has been produced yet. Solutions from deployment 66 looks the most benign with the smallest RMS against mooring SSH. For deployment 63, at around 8 pm, 11th Dec, 2020, the buoy dragged its anchor in rough sea state and drifted away from the JAS CP. Lighter shade of colour in each panel represent outliers in the solutions.

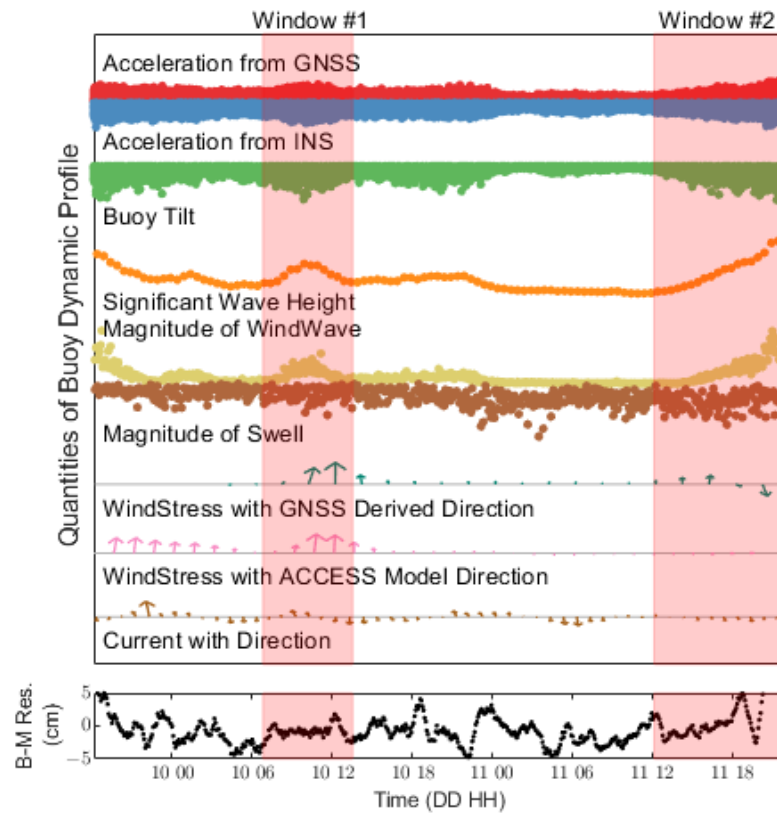


Figure S7. Dynamic Profiles of the Buoy based on Observations and Model for Deployment 63. In the upper panel, quantities are provided without detailed magnitude on the y-axis for all indicators as the time correlation is the focus of the figure rather than their absolute values. Acceleration from INS is from the 100-Hz sampling of an accelerometer on-board. A 2-Hz moving mean window is applied on the raw acceleration from INS to reduce the systematic noise of the unit. Buoy tilt is in the unit of cosine of the tilting in degrees and calculated based on IMU derived roll and pitch of the platform. Magnitudes of waves are normalized within [0,1] based on their range separately, hence they are not suitable for quantitative inter-comparison. Wind stress comes from ACCESS-G model, with a temporal resolution of 1 hour and spatial resolution of ~12 km. Wind stress with GNSS derived direction is plotted as a combination of GNSS wave direction and wind stress amplitude from the ACCESS model – interpolated to 1.5 hours in the figure. Quivers of the wind stress with ACCESS model direction are directly plotted as from the model. Currents are observed by the in situ current-meter with a sampling rate of 20-min. The directions are further down sampled to 1 hour in this figure. Quivers of the current showed tidal behaviour in both amplitude and direction. In the lower panel, buoy minus mooring residuals is shown. Two possible weather windows have been labelled. In window #1, the local wind picked up, which further excited the buoy dynamics as evidenced in the accelerations, and buoy tilt. It can also be shown in the derived SWH and the modelled wind stress. In Window #2, the wind continued to pick up till the end of the deployment.

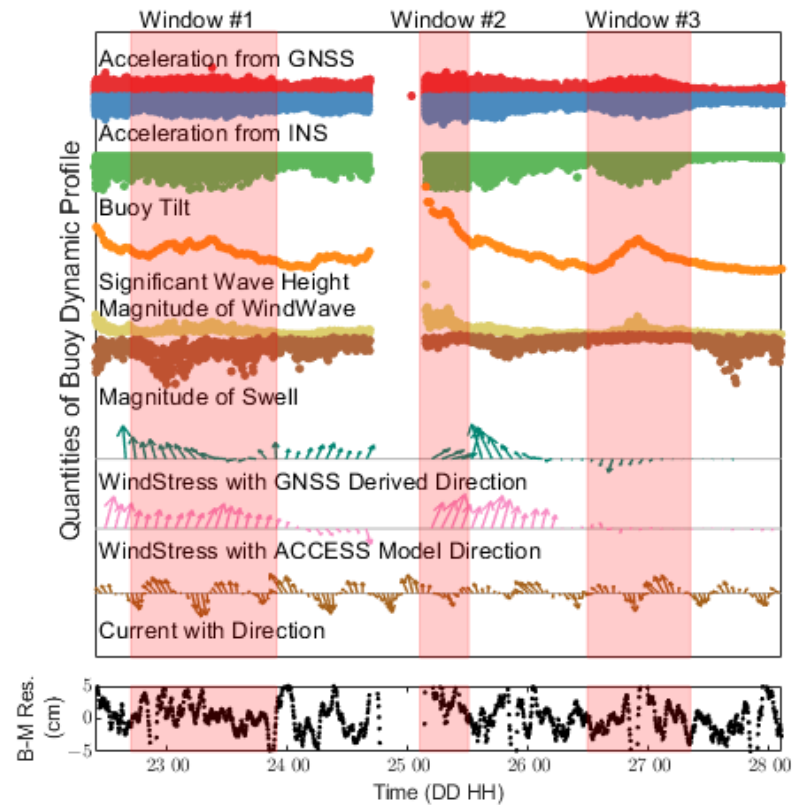


Figure S8. Dynamic Profiles of the Buoy based on Observations and Model for Deployment 64. Figure conventions are the same as described in Figure S7. Wind stress quivers are interpolated to 2 hours in the figure, while current quivers are down sampled to 1 hour. Three windows have been labelled. In window #1, an energy from far field propagates the energy to the buoy location as shown in the swell time series, which further excited the acceleration and the tilt. Prior to window #2, there was a signal loss followed by some diverged solutions in the buoy system, possibly due to some high sea state condition flushing water over the antenna. The high sea state is evident in both the derived SWH and the modelled wind stress within the window. In window #3, an isolated local wind picked up, lasting for a short period of time.

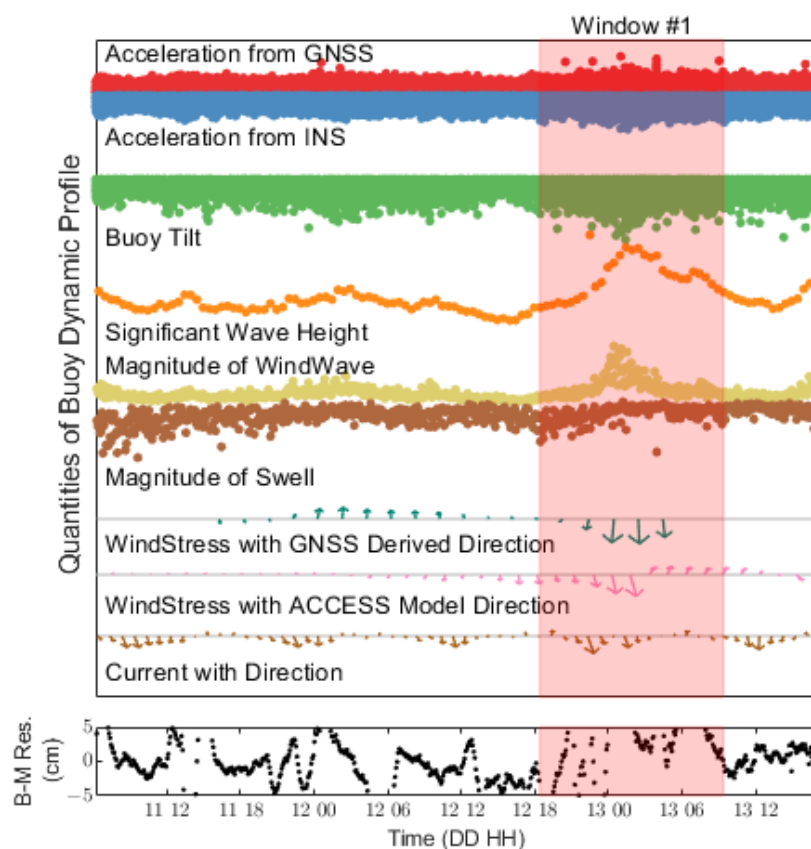


Figure S9. Dynamic Profiles of the Buoy based on Observations and Model for Deployment 65. Figure conventions are the same as described in Figure S7. Wind stress quivers are interpolated to 1.5 hours in the figure, while current quivers are down sampled to 1 hour. Only one window has been labelled, in which a local windy condition was observed by the buoy as indicated in multiple derived quantities as well as the wind stress model.